PHYSICAL REVIEW D **88,** 113003 (2013)

Supersimple analysis of $e^-e^+ \to W^-W^+$ at high energy

G. J. Gounaris[1] and F. M. Renard[2]

[1]*Department of Theoretical Physics, Aristotle University of Thessaloniki, Gr-54124 Thessaloniki, Greece*
[2]*Laboratoire Univers et Particules de Montpellier, UMR 5299, Université Montpellier II, Place Eugène Bataillon CC072, F-34095 Montpellier Cedex 5, France*

(Received 13 September 2013; published 5 December 2013)

Studying $e^-e^+ \to W^-W^+$ at the one-loop electroweak order, we derive very accurate and simple expressions for the four helicity conserving amplitudes which dominate this process at high energies. The calculations are done in both the standard model and minimal supersymmetric standard model frameworks. Such expressions, called supersimple, nicely emphasize the dynamical contents of each framework. Numerical illustrations are presented, which show the accuracy of this description, and how it can be used for identifying possible additional new physics contributions, like, e.g., anomalous gauge couplings or a new Z' vector boson exchange. The procedure is useful even if only the standard model is visible at the future linear collider energies.

DOI: 10.1103/PhysRevD.88.113003 PACS numbers: 12.15.−y, 12.15.Lk, 12.60.Jv, 13.66.Fg

I. INTRODUCTION

The process $e^-e^+ \to W^-W^+$ has been studied theoretically and experimentally since a long time, as it provides sensitive tests of the gauge structure of the electroweak interactions [1–4] and checks the possible presence of nonstandard new physics contributions. A detailed history of the subject and a list of references may be seen in [4].

First, experimental studies of this process have been done at LEP2 [5]. No signal of departures from the standard model (SM) has been found, but the accuracy is not sufficient to eliminate the possibility of new physics effects at a high scale.

LHC studies involving production of W pairs also exist; but their detailed studies require a difficult event analysis because of various sources of background [6].

Future high energy e^-e^+ colliders are therefore deeply desired in order to provide fruitful information about this subject [7,8].

From the theoretical side, the present situation of a one-loop electroweak (EW) order analysis, aiming, e.g., at searching for any nonstandard effects, is quite complex. This is already true at the SM level, and if one includes SM extensions like, e.g., supersymmetry (SUSY), the sensitivity to any benchmark choice has to be considered. Particularly for amplitudes involving longitudinal W's, the numerical situation is more difficult, because of the huge cancellations taking place. In both the SM and SUSY cases, very lengthy numerical codes are required to describe the complete one-loop EW contribution; see, e.g., [3,4].

The aim of the present paper is to call attention to the fact that at high energies, the one-loop EW corrections to the helicity amplitudes for $e^-e^+ \to W^-W^+$ acquire very simple forms in both the SM and minimal supersymmetric standard model (MSSM) cases. To establish them we have done a complete calculation of the one-loop diagrams and then taken the high energy, fixed angle limit using [9]. The soft photon bremsstrahlung can then be added as usual [1–4].

Our procedure is the same as the one used previously for other 2-to-2 processes, leading to the "supersimple" (sim) one-loop EW expressions for the dominant high energy helicity conserving (HC) amplitudes; the helicity violating (HV) ones are quickly vanishing[1] [10,11]. We find very simple and quite accurate expressions for the high energy HC amplitudes, in both the SM and MSSM frameworks, which nicely show their relevant dynamical contents.

The use of this description, which clearly indicates the relevant physical parameters, should very much simplify the analysis of the experimental results. Particularly because its accuracy turns out to be sufficient for distinguishing one-loop SM (or MSSM) effects, from, e.g., various types of additional new physics contributions, like anomalous gauge couplings (AGCs) or Z' exchange; see, for example, [12].

The content of the paper is the following. In Sec. II we present the various properties of the high energy $e^-e^+ \to W^-W^+$ amplitudes, with special attention to their helicity conservation (HCsn) property [13,14]. The explicit supersimple expressions are discussed in the later part of Sec. II and in Appendix A. In Sec. III we present the energy and angular dependencies of the cross sections, for polarized and unpolarized electron beams, in either the SM or MSSM. And subsequently, we compare these SM or MSSM contributions to those due to anomalous gauge couplings (AGC) or Z' effects; both given in Appendix B. We find that the accuracy of the supersimple expressions is sufficient for distinguishing these various types of contributions. Thus, they may be used instead of the complete one-loop results. The conclusions summarize these results.

[1]The notations HC and HV are fully defined in the next section.

II. SUPERSIMPLICITY IN $e^-e^+ \to W^-W^+$

The process studied to the one-loop EW order is

$$e^-_\lambda(l)e^+_{\lambda'}(l') \to W^-_\mu(p)W^+_{\mu'}(p'), \tag{1}$$

where (λ, λ') denote the helicities of the incoming (e^-, e^+) states, and (μ, μ') the helicities of the outgoing (W^-, W^+). The corresponding momenta are denoted as (l, l', p, p'). Kinematics are defined through

$$s = (l + l')^2 = (p + p')^2, \qquad t = (l - p)^2 = (l' - p')^2,$$
$$p_W = \sqrt{\frac{s}{4} - m_W^2}, \qquad \beta_W = \sqrt{1 - \frac{4m_W^2}{s}}, \tag{2}$$

where p_W, β_W denote, respectively, the $W^\mp$ three-momentum and velocity in the W^-W^+-rest frame. Finally, the angle between the incoming e^- momentum l and the outgoing W^- momentum p, in the center of mass frame, is denoted as θ.

Because of the smallness of the electron mass, non-negligible amplitudes at high energies only appear for $\lambda = -\lambda' = \mp 1/2$. The helicity amplitudes for this process are therefore determined by three helicity indices and are denoted as $F_{\lambda,\mu,\mu'}(\theta)$, where (e^-, W^-) are treated as particles No. 1, and (e^+, W^+) as particles No. 2, in the standard Jacob-Wick notation [15].

Assuming CP invariance, we obtain the constraint

$$F_{\lambda,\mu,\mu'}(\theta) = F_{\lambda,-\mu',-\mu}(\theta), \tag{3}$$

which means that the process is described by just 12 independent helicity amplitudes.

At high energy, the HCns rule implies that only the amplitudes satisfying

$$\lambda + \lambda' = 0 = \mu + \mu' \tag{4}$$

can dominate [13,14]. These are the HC amplitudes, which explicitly are

$$F_{\mp-+}, \qquad F_{\mp+-}, \qquad F_{\mp 00}. \tag{5}$$

The purely left-handed W couplings though forces the HC amplitudes

$$F_{++-}, \qquad F_{+-+}, \tag{6}$$

to vanish at the Born level and be very small at one-loop. Thus, only four leading HC helicity amplitudes remain at high energy, namely,

$$F_{--+}, \qquad F_{-+-}, \qquad F_{\pm 00}. \tag{7}$$

The remaining amplitudes, which violate (4), are termed as HV ones. Explicitly these are

$$\begin{matrix} F_{-0+}, & F_{---}, & F_{-+0}, \\ F_{+0+}, & F_{+--}, & F_{++0}, \end{matrix} \tag{8}$$

and are expected to be suppressed like $m_W/\sqrt{s}$ or m_W^2/s, at high energy.

A. Born contribution to the helicity amplitudes

We next turn to the Born contribution to the HC and HV amplitudes in (7) and (8), respectively. The relevant diagrams involve neutrino exchange in the t channel and photon + Z exchange in the s channel. The resulting amplitudes satisfy the HCns constraints [13,14]. In the usual Jacob and Wick convention [15], their exact expressions are

Transverse-transverse (TT) amplitudes $(\mu, \mu' = \pm 1)$

Using (2), we find

$$\begin{aligned} F^{\text{Born}}_{\lambda\mu\mu'} = {} & \frac{se^2 \sin\theta}{16ts_W^2}\delta_{\lambda,-}\{\mu + \mu' + \beta_W(1 + \mu\mu') \\ & - 2\mu(1 + \mu'\cos\theta)\} \\ & + \frac{se^2}{4}\left[\frac{Q_e}{s} + \frac{a_{eL}\delta_{\lambda,-} + a_{eR}\delta_{\lambda,+}}{2s_W^2(s - m_Z^2)}\right] \\ & \times (1 + \mu\mu')(2\lambda)\beta_W \sin\theta, \end{aligned} \tag{9}$$

with

$$Q_e = -1, \qquad a_{eL} = 1 - 2s_W^2, \qquad a_{eR} = 2s_W^2, \tag{10}$$

determining the electron charge, and the Z left and right couplings. Because of the purely left-handed W coupling, Eq. (9) leads to

$$F^{\text{Born}}_{+\frac{1}{2}\mu,-\mu} = 0, \tag{11}$$

as already said just after (6). In addition, (9) leads at high energy to

$$F^{\text{Born}}_{\lambda\mu\mu} \to 0, \tag{12}$$

in agreement with HCns [13,14], and

$$F^{\text{Born}}_{-\frac{1}{2}\mu-\mu} \to -\frac{e^2 \sin\theta(\mu - \cos\theta)}{4s_W^2(\cos\theta - 1)}. \tag{13}$$

This confirms that the first two HC Born amplitudes in (7) go to constants asymptotically.

Transverse-longitudinal (TL) and longitudinal-transverse (LT) amplitudes $(\mu = \pm 1,\ \mu' = 0,\ \mu = 0,\ \mu' = \pm 1)$

Using again (2), we obtain

$$\begin{aligned} F^{\text{Born}}_{\lambda\mu 0} = {} & \frac{s\sqrt{s}e^2}{8\sqrt{2}m_W t s_W^2}\delta_{\lambda,-}\Big\{(\beta_W - \cos\theta)(1 - \mu\cos\theta) \\ & - \frac{2m_W^2}{s}(\mu - \cos\theta)\Big\} - \frac{s\sqrt{s}e^2}{2\sqrt{2}m_W}\Big[\frac{Q_e}{s} \\ & + \frac{a_{eL}\delta_{\lambda,-} + a_{eR}\delta_{\lambda,+}}{2s_W^2(s - m_Z^2)}\Big]\beta_W(1 + 2\lambda\mu\cos\theta), \end{aligned} \tag{14}$$

$$F^{\text{Born}}_{\lambda 0\mu'} = \frac{s\sqrt{s}e^2}{8\sqrt{2}m_W t s_W^2}\delta_{\lambda,-}\Big\{(\beta_W - \cos\theta)(1+\mu'\cos\theta) - \frac{2m_W^2}{s}(\mu' + \cos\theta)\Big\} - \frac{s\sqrt{s}e^2}{2\sqrt{2}m_W}\Big[\frac{Q_e}{s} + \frac{a_{eL}\delta_{\lambda,-} + a_{eR}\delta_{\lambda,+}}{2s_W^2(s-m_Z^2)}\Big]\beta_W(1 - 2\lambda\mu'\cos\theta). \quad (15)$$

The amplitudes in (14) and (15) are both HV, and at high energies they are quickly suppressed like $m_W/\sqrt{s}$.

The *longitudinal-longitudinal (LL) amplitudes* ($\mu = 0$, $\mu' = 0$) are

$$F^{\text{Born}}_{\lambda 00} = \frac{se^2\sin\theta}{16ts_W^2}\delta_{\lambda,-}\Big\{\frac{s}{m_W^2}(\beta_W - \cos\theta) + 2\beta_W\Big\} + \frac{(2\lambda)s^2e^2}{8m_W^2}\Big[\frac{Q_e}{s} + \frac{a_{eL}\delta_{\lambda,-} + a_{eR}\delta_{\lambda,+}}{2s_W^2(s-m_Z^2)}\Big] \times \beta_W(3-\beta_W^2)\sin\theta, \quad (16)$$

where (2) have again been used. At high energy, keeping terms to order m_Z^2/s and m_W^2/s, one gets

$$F^{\text{Born}}_{-\frac{1}{2}00} \to -\frac{e^2}{8s_W^2c_W^2}\sin\theta, \qquad F^{\text{Born}}_{+\frac{1}{2}00} \to \frac{e^2}{4c_W^2}\sin\theta, \quad (17)$$

which, together with (13), confirm that all Born HC amplitudes in (7) go to constants asymptotically. On the contrary, all six HV amplitudes listed in (8) vanish, in this limit.

The Born level properties of the helicity amplitudes are illustrated in Fig. 1. The two HC amplitudes listed in (6) are not shown since they vanish when coefficients proportional to the electron mass are neglected.

B. Helicity amplitudes to the one-loop EW order

The relevant contributions come from up and down triangle diagrams in the t channel; initial and final triangle diagrams in the s channel; direct, crossed, and twisted box diagrams; specific triangles involving a 4-leg gauge boson couplings; and finally neutrino, photon and Z self-energies. Counterterms in the Born contributions, which help cancelling the divergences induced by self-energy and triangle diagrams, are also included, leading to the so-called on-shell renormalization scheme [16].

Such types of computations have already been done; see, for example, [3,4]. But our aim here is to look at the specific properties of each of the helicity amplitudes, and to derive simple high energy expressions for the HC ones. For this reason we repeated the complete calculation of the one-loop EW corrections and then computed their high energy expressions that we call sim, using the expansion of [9]. A special attention is paid to the virtual photon exchange diagrams leading to infrared singularities (when $m_\gamma \to 0$) which are then cancelled by the addition of the soft photon bremsstrahlung contribution. The sim expressions are given (in Appendix A) in the two possible choices, arbitrary small m_γ value, or $m_\gamma = m_Z$ which can be considered as "small" at high energies. This second choice, also used in previous studies [10,11], has the advantage of leading to even simpler expressions as we can see in Appendix A.

As already said and numerically shown below, the HV amplitudes in (8) are negligible at high energies. Only the four HC amplitudes appearing in (7) are relevant there. Turning to them, we present in Appendix A 1 the very simple sim expressions for the TT amplitudes F_{--+}, F_{-+-}; while the corresponding expressions for the LL amplitudes F_{-00}, F_{+00} appear in Appendix A 2. The results, (A8), (A9), (A13), and (A14) give the SM predictions, while, (A10), (A11), (A15), and (A16) give the MSSM ones, always corresponding to the $m_\gamma = m_Z$ choice. The corrections to be done to them in order to obtain the general result for any m_γ, appear in (A12) and (A17).

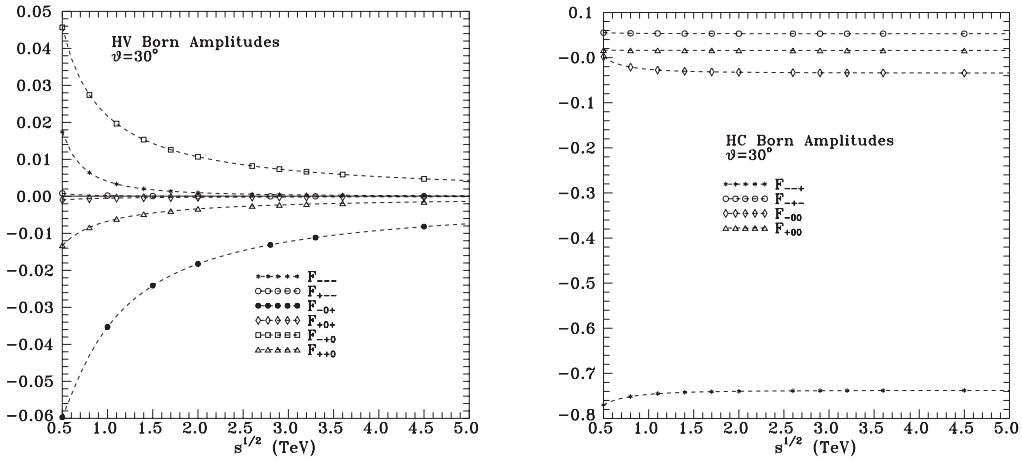

FIG. 1. Left panel: Born contributions to the six HV amplitudes listed in (8). Right panel: Born contributions to the the four HC amplitudes listed in (7).

For deriving these, we start from the complete one-loop EW results in terms of Passarino-Veltman functions [17], and then use their high energy expansions given in [9]. For the TT amplitudes F_{--+}, F_{-+-}, the derivation is quite straightforward.

For the two LL amplitudes F_{-00}, F_{+00} though, the derivation is very delicate, because of huge gauge cancellations among contributions exploding like[2] s/m_W^2. Such cancellations also occur at the Born level, between t- and s-channel terms. But at one-loop level, the situation is much more spectacular, because more diagrams are involved. Technically, the derivation of the limiting expressions can be facilitated by using the equivalence theorem and looking at the Goldstone process $e^-e^+ \to G^-G^+$ [19].

We next turn to the infrared divergencies implied by the presence of m_γ in the $e^-e^+ \to W^-W^+$ amplitudes. As usual, these are canceled at the cross section level by adding to the one-loop EW results for $d\sigma(e^-e^+ \to W^-W^+)/d\Omega$, the Born-level cross section describing the soft photon bremsstrahlung, given by

$$\frac{d\sigma_{\rm brems}(e^-e^+ \to W^-W^+\gamma)}{d\Omega} = \frac{d\sigma^{\rm Born}(e^-e^+ \to W^-W^+)}{d\Omega}\,\delta_{\rm brems}(m_\gamma, \Delta E), \quad (18)$$

where $\delta_{\rm brems}(m_\gamma, \Delta E)$ is given by[3] Eq. (5.18) in [1], while ΔE describes the highest energy of the emitted unobservable soft photon, satisfying

$$m_\gamma \le \Delta E \ll \sqrt{s}. \quad (19)$$

The only requirement for this cancellation to happen is that m_γ is *small*; i.e., that terms proportional to a power of m_γ (not inside a high energy logarithm) are always negligible. Under these conditions, any m_γ dependence cancels out in the sum $d\sigma(e^-e^+ \to W^-W^+)/d\Omega$ plus $d\sigma_{\rm brems}/d\Omega$.

But, at the high energies of $\sqrt{s} \gg m_Z$ we are interested in, the Z mass is also *small*, since any such m_Z coefficient is necessarily suppressed by an energy denominator. In other words, since the infrared m_γ effects cancel out in the cross section including the bremsstrahlung (18) contribution, they will also cancel in the special case $m_\gamma = m_Z$. As already said, we made this choice because it leads to the simplest expressions. The illustrations given below correspond to it.

In order to obtain the (infrared sensitive) unpolarized cross section $d\sigma(e^-e^+ \to W^-W^+)/d\Omega$ from the experimental data, one has obviously to subtract the bremsstrahlung contribution. Consequently, the difference between the values of this cross section regularized at an arbitrary m_γ or at $m_\gamma = m_Z$, for the same ΔE, is given by

$$\left.\frac{d\sigma(e^-e^+ \to W^-W^+)}{d\Omega}\right|_{m_\gamma} - \left.\frac{d\sigma(e^-e^+ \to W^-W^+)}{d\Omega}\right|_{m_\gamma \to m_Z} = \frac{d\sigma^{\rm Born}}{d\Omega}\frac{\alpha}{\pi}\left(\ln\frac{m_Z}{m_\gamma}\right)\left(4 - 2\ln\frac{s}{m_e^2} + 4\ln\frac{m_W^2 - u}{m_W^2 - t} + 2\frac{s - 2m_W^2}{s\beta_W}\ln\frac{1-\beta_W}{1+\beta_W}\right); \quad (20)$$

see our Eqs. (2) and (18) and Eq. (5.18) of [1]. If one wants to keep the usual choice of an arbitrary small m_γ in the bremsstrahlung cross section, one would have to use our extended sim expressions given in (A12) and (A17) of Appendix A.

Turning now to the numerical illustrations, we first check that all HV amplitudes quickly vanish at high energy, in both MSSM and SM [13,14]. For the MSSM case, we use benchmark S1 of [20], where the EW scale values of all squark masses are at the 2 TeV level, $A_t = 2.3$ TeV, the slepton masses are at 0.5 TeV, and the remaining mass parameters (in TeV) are

$$\mu = 0.4, \qquad M_1 = 0.25, \qquad M_2 = 0.5, \qquad M_3 = 2, \quad (21)$$

while $\tan\beta = 20$. Such a benchmark is consistent with present LHC constraints [20]. All MSSM results shown in this paper are using this benchmark. Similar results are also obtained for other LHC-consistent MSSM benchmarks, like those listed, e.g., in the Snowmass suggestion [21] or the very encouraging cMSSM ones given in [22].

Comparing the SM and MSSM results in Fig. 2, we see that for all HV amplitudes, the purely supersymmetric contribution mostly cancel the (already suppressed) pure SM ones; this is more spectacular for energies above the SUSY scale. Thus, Fig. 2 indeed shows that the six HV amplitudes listed in (8), are quickly suppressed in the MSSM, as well as in the SM.

We next turn to the high energy description of the four leading (HC) amplitudes listed in (7). As it is shown in Fig. 3, the sim approximations to them follow very closely the complete expressions for the one-loop electroweakly corrected amplitudes in both SM and MSSM. For the TT amplitudes F_{--+}, F_{-+-}, this appears in the upper panels of Fig. 3, for the SM and the MSSM benchmark mentioned above. The corresponding numerical illustrations for the LL HC amplitudes are shown in the lower panels. These results indicate that all four one-loop predictions, i.e., the complete SM and MSSM results, as well their sim SM and sim MSSM approximations, are very close to each other at

[2]Particularly for neutralinos, this demands a very accurate determination of their mixing matrices, like the one supplied, e.g., by [18].

[3]Parameter λ in [1] corresponds to our m_γ.

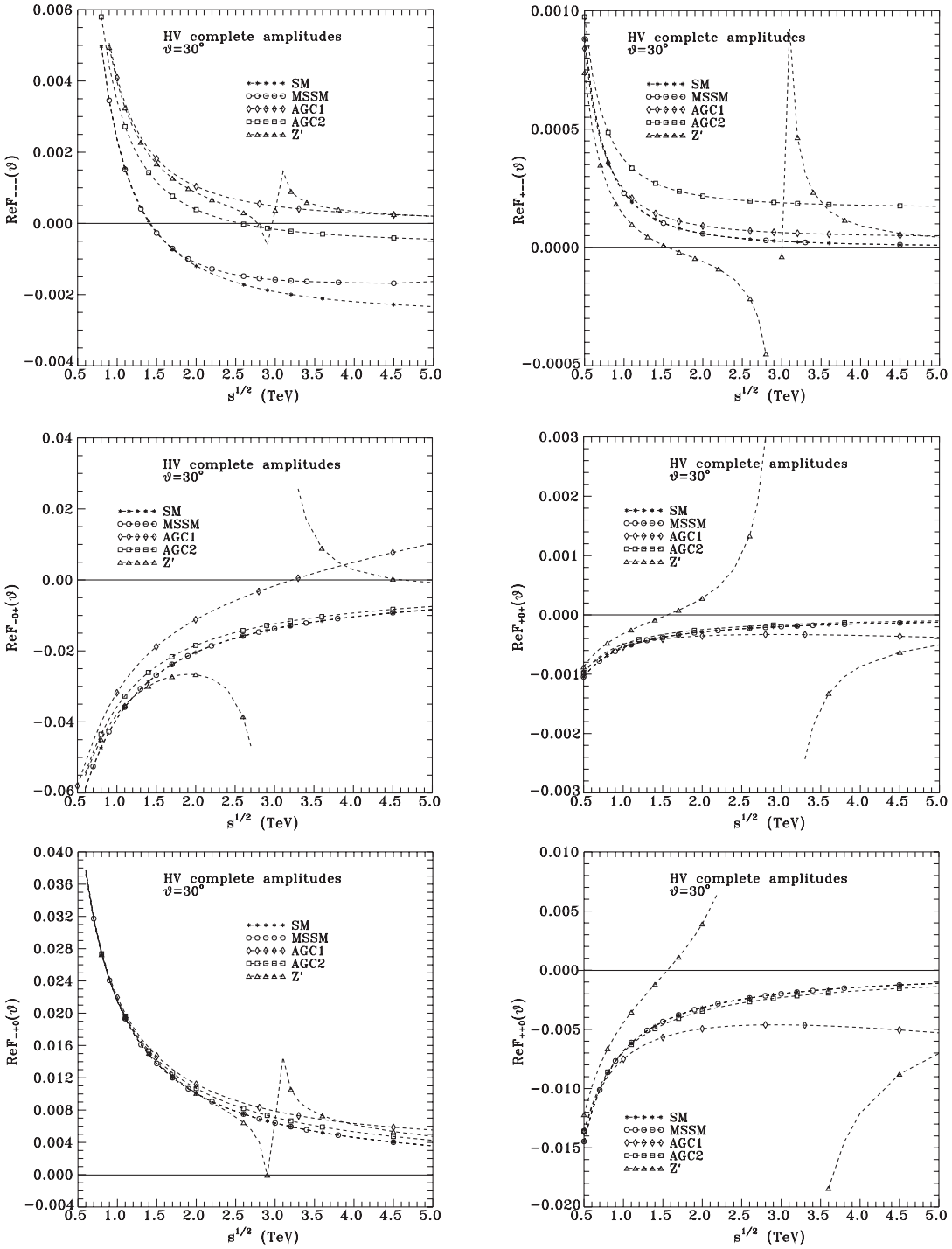

FIG. 2. The real parts of the six HV amplitudes listed in (8), at one-loop EW order in the SM and MSSM, using the $m_\gamma = m_Z$ regularization. The new physics contributions from AGC1, AGC2, or a new Z' (see text) are also shown. The horizontal solid lines indicate how these HV amplitudes compare to a vanishing asymptotic value expected in the MSSM. The imaginary parts of the amplitudes are much smaller since they receive no Born contribution.

high energies. Moreover, a comparison of Figs. 2 and 3 immediately shows that soon above 0.5 TeV the HC amplitudes in (7) are much larger than all other ones.

There are two main conclusions we draw from this, for energies up to a TeV or so: The first is that the process $e^-e^+ \to W^-W^+$ is rather insensitive to MSSM contributions for benchmarks consistent with the present SUSY constraints [20–22]. And the second conclusion is that, (A8), (A9), (A13), and (A14) provide a true description of the sources of the relevant dynamics.

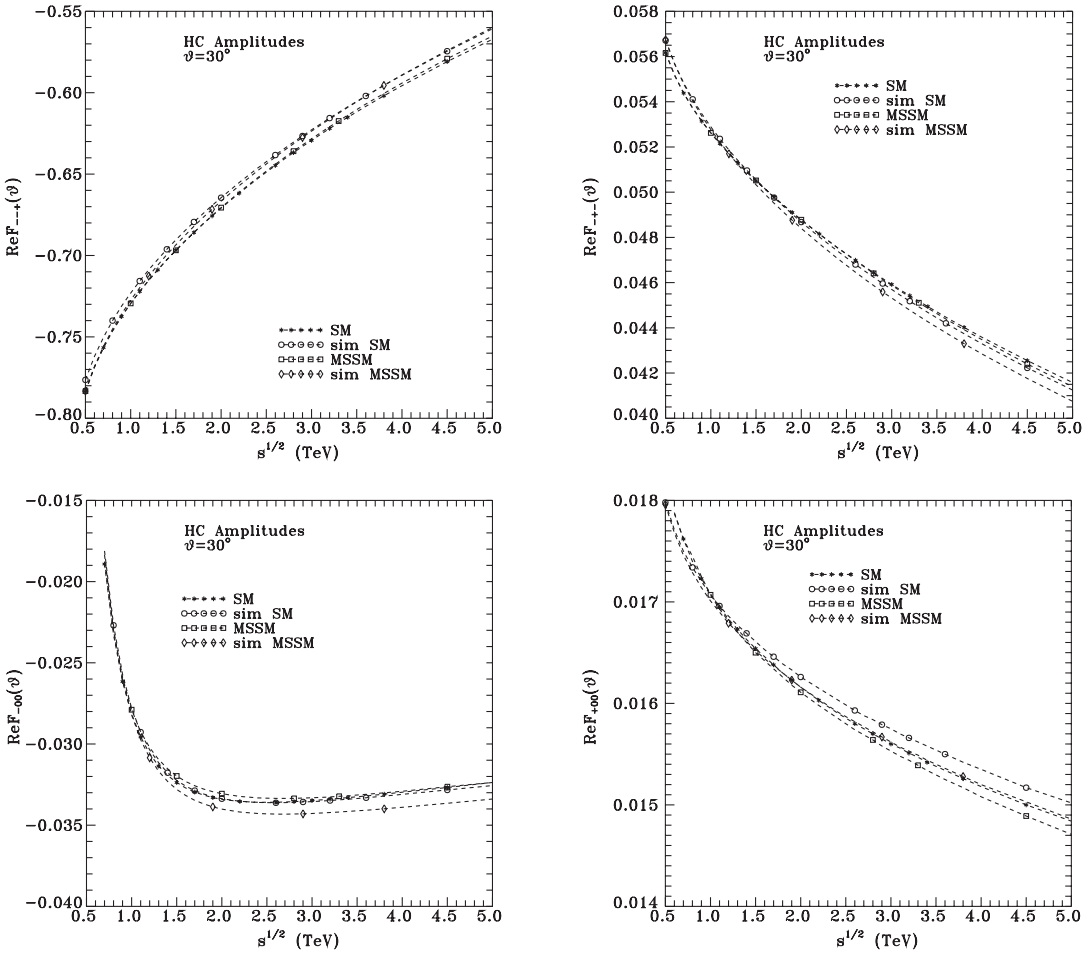

FIG. 3. The real parts of the complete one-loop EW results for the four HC amplitudes listed in (7), and their sim approximations, in the SM and the MSSM benchmark described in the text. Upper (lower) panels describe the TT (LL) amplitudes, respectively. The imaginary parts of the amplitudes are much smaller since they receive no Born contribution.

III. APPLICATION TO THE $e^-e^+ \to W^-W^+$ OBSERVABLES

The observables we study here are the unpolarized differential cross sections

$$\frac{d\sigma}{d\cos\theta} = \frac{\beta_W}{128\pi s}\Sigma_{\lambda\mu\mu'}|F_{\lambda\mu\mu'}(\theta)|^2, \tag{22}$$

as well as the polarized differential cross sections using right-handedly polarized electron beams e_R^-,

$$\frac{d\sigma^R}{d\cos\theta} = \frac{\beta_W}{64\pi s}\Sigma_{\mu\mu'}|F_{+\frac{1}{2},\mu\mu'}(\theta)|^2, \tag{23}$$

where (2) is used.

These cross sections are shown in Fig. 4, where the complete one-loop EW order SM results are compared to the corresponding sim ones. The later are constructed by using the expressions of Appendix A for the HC amplitudes, while the HV amplitudes are approximated by the quickly vanishing Born contributions[4] in (9), (14), and (15). As shown in Fig. 4, the sim results very closely follow the SM ones.

In addition, we show in the same figure how the complete one-loop SM results are changed when an anomalous contribution is added like, e.g., AGC1 or AGC2, respectively, defined by (B5) or (B6) and (B7) of Appendix B 1; or a Z' effect defined in Appendix B 2.

The left panels in Fig. 4 present results for the unpolarized e^-e^+ cross sections; while the right panels show results for the $e_R^-e^+$ cross sections involving a right-handedly polarized electron.

The upper panels present the energy dependencies at $\theta = 30^o$; while the middle (lower) panels indicate the angular dependencies at $\sqrt{s} = 1$ TeV ($\sqrt{s} = 5$ TeV).

[4]If instead we had completely ignored the HV amplitudes in the sim cross sections, then appreciable differences would only appear for energies below 1 TeV, particularly for the e_R^- cross sections.

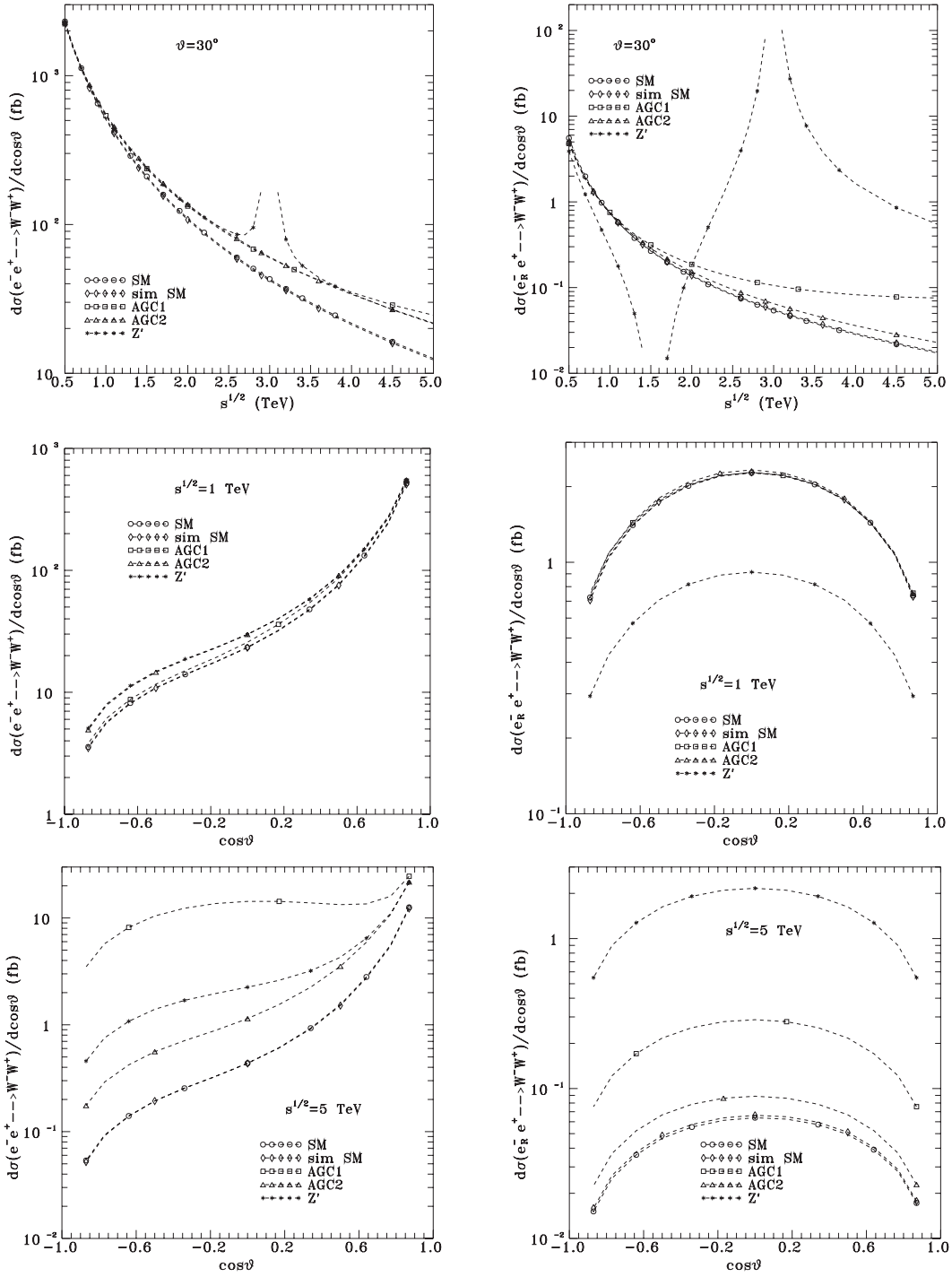

FIG. 4. Differential cross sections for unpolarized $e^- e^+$ (left panels), and right-electron polarized $e_R^- e^+$ (right panels), in the SM, sim SM, and some new physics models (see text). Upper panels show the energy dependencies at $\theta = 30^o$. Middle (lower) panels give the angular dependencies at $\sqrt{s} = 1$ TeV ($\sqrt{s} = 5$ TeV).

In all cases, the sim description is very good. No MSSM or sim MSSM illustrations are given since they are very close to the corresponding SM ones: at the 1%–2% level, for benchmarks consistent with the current LHC constraints [20–22].

In other words, at the scale of Fig. 4, the SM and MSSM results for [20] would coincide. Such a weakness of the pure supersymmetric contributions, has been already noticed in previous analyses [3]. Because of the different mass scales of the supersymmetric partners, at a given energy, the absolute magnitudes of the SUSY one-loop effects may differ notably. But relative to the SM contributions (Born + one − loop), they always remain very small.

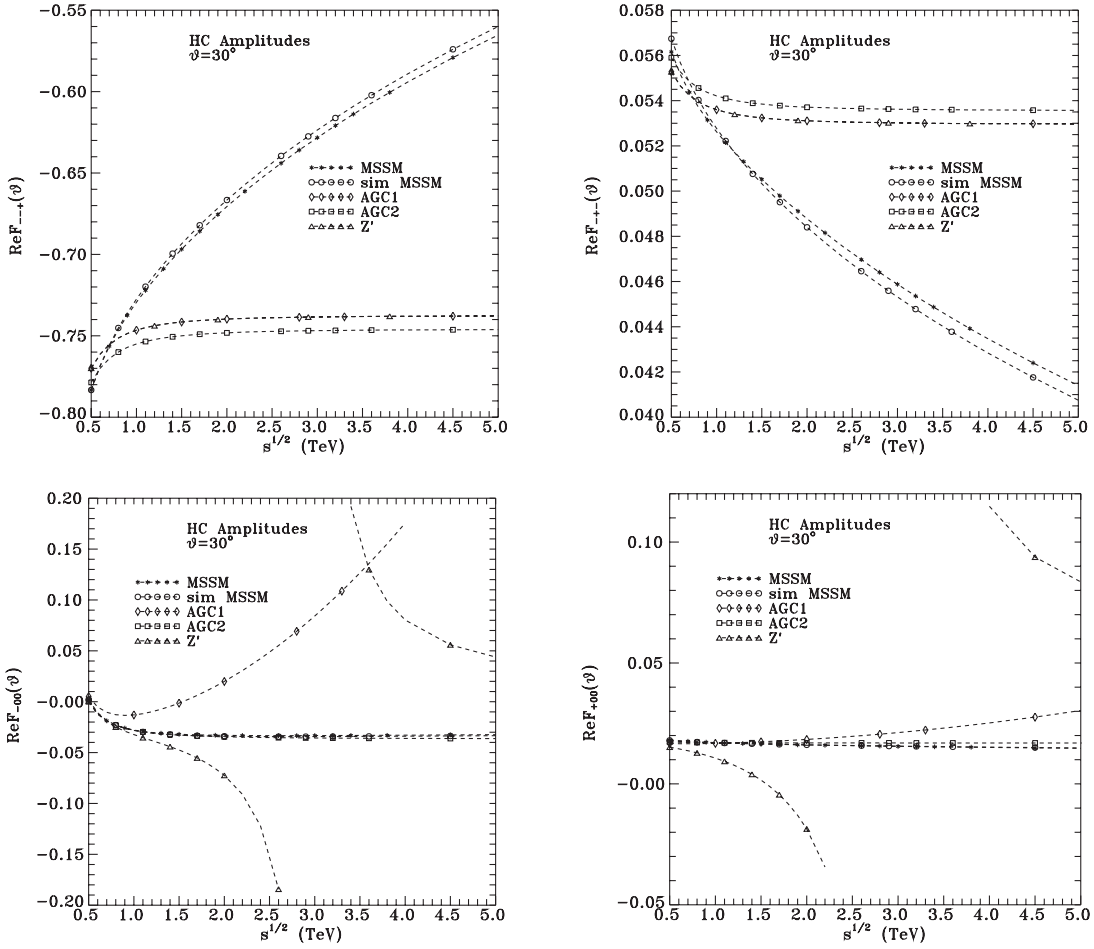

FIG. 5. The complete one-loop EW contributions to the real parts of the four HC amplitudes listed in (7), and their sim approximations, in the MSSM benchmark described in the text; (as shown in Fig. 3, the SM and MSSM results are very close to each other). The new physics AGC1, AGC2, and Z' results are also presented. Upper (lower) panels describe the TT (LL) amplitudes, respectively. Imaginary parts of the amplitudes are much smaller and they are not shown.

Concerning the relevant dynamics for the unpolarized e^-e^+ cross sections, we note that at forward angles they are dominated by the left-handed-e^- TT amplitudes.

For specific experimental studies of the LL amplitudes, one can either make a final polarization analysis of the $W^\mp$ decays, or use a right-handedly polarized e^- beam so that the usual TT amplitudes do not contribute. In the right panels in Fig. 4, we show the energy and angular dependencies of these $e_R^- e^+$ cross sections.

These LL studies are probably the best place to search for anomalous contributions, like those from the AGC effects presented in Sec. B 1. As seen in (B1)–(B4), such AGC contributions do not appear in the HC TT amplitudes; but, they do appear in the HC LL amplitudes, as well as in all the HV ones (TT, TL, and LT). This is a remarkable property that should be checked by a careful analysis of experimental signals.

The most simple-minded implication of AGC physics is presented by the AGC1 model in Figs. 2, 4, and 5, where the parameters in Appendix B 1 are fixed as in (B5). In this case, the anomalous contributions to the LL amplitudes increase like s/m_W^2, causing a strong increase of the cross sections with the energy.

Such a strong increase may be tamed though, by the existence of scales M in the various anomalous couplings, which transforms them to form factors decreasing like $M^2/(s+M^2)$.

Another way of taming the above strong AGC increase is by the addition of new exchanges in the t channel, such that one gets cancellations between s- and t-channel contributions, like in the Born SM case. A purely *ad hoc* phenomenological solution of this kind is given by AGC2, presented in Appendix B 1, and determined by (B6) and (B7). In the effective Lagrangian framework many such possibilities exist; see, e.g., [23].

The AGC1 and AGC2 results in Figs. 2, 4, and 5, show various amplitudes and cross sections where such anomalous behaviors may be seen and compared to the SM and MSSM results.

Present experimental constraints on fixed AGC couplings, from LEP2 [5] are of the order of ± 0.04. From LHC [6], they are of the order of ± 0.1; compare with (B5) and (B7). These values are much larger than the uncertainties of our description.

Another type of anomalous contribution is a Z' exchange in the s channel; see [12] and Appendix B 2. Here also one can impose a good high energy behavior to the LL and LT amplitudes. A simple solution is a Z-Z' mixing such that the total s-channel contribution at high energy cancels the standard t-channel exchange at the Born level. Figures 2, 4, and 5 show the behaviors of the various amplitudes and cross sections under the presence of such Z' contributions and compare them to the corresponding SM and MSSM ones.

From the above illustrations one sees that our supersimple expressions are sufficiently accurate to distinguish one-loop SM or MSSM corrections from such new physics. But these are examples. More elaborated analyses could of course be done, for example, in the spirit of [12], still remaining in a sensitivity region where supersimple expressions sufficiently describe SM physics. The existence of this possibility constitutes an important motivation for supersimplicity.

IV. CONCLUSIONS

In this paper we have analyzed the high energy behavior of the one-loop EW corrections to the $e^-e^+ \to W^-W^+$ helicity amplitudes. And we have verified that soon above threshold, the four helicity conserving amplitudes in (7) are much larger than all other ones, in both the SM and MSSM.

We have then established the so-called sim expressions for the HC amplitudes in (7), both in the SM and in MSSM. These expressions (explicitly written in Appendix A) are really simple and provide a panoramic view of the dynamics, i.e., of the fermion, gauge, and Higgs exchanges, and (in the supersymmetric part) of the sfermion, additional Higgses, charginos, and neutralinos exchanges.

Moreover, the accuracy of these sim expressions is sufficient to allow their use in order to search for possible new physics contributing, in addition, to the SM or MSSM. In other words, sim expressions may be used to avoid the enormous codes needed when using the complete one-loop expressions. Thus, analyses done by only using Born terms can be easily upgraded to the one-loop EW order.

In previous work [10,11], we have emphasized the peculiar simplicity arising in the MSSM case. However in the process $e^-e^+ \to W^-W^+$, the purely supersymmetric contributions are rather small. So even in the purely SM case, we get simple accurate expressions that are valid at LHC energies.

At present there is no signal of supersymmetry at LHC. The discovery of the Higgs boson at 125 GeV is nevertheless a source of questions about the possibility of various kinds of new physics effects [24]. The process $e^-e^+ \to W^-W^+$ is a typical place where such effects can be looked for. For our illustrations, we have taken the cases of AGC or Z' contributions, which have been often discussed. Other possibilities may of course be tried [12].

Our supersimple expressions are intended to help differentiating such new physics effects from standard or supersymmetric corrections, in a way which is as simple as possible, while at the same time allowing us to directly see the responsible dynamics.

APPENDIX A: SUPERSIMPLE EXPRESSIONS FOR THE FOUR HC AMPLITUDES

The purpose of this appendix is to present the sim expressions for the four leading HC amplitudes listed in (7). The procedure is valid for of any 2-to-2 process at one-loop EW order, in either MSSM or SM, provided the Born contribution is non-negligible. And it is based on the fact that the HC amplitudes, are the only relevant ones at high energy [13,14].

To derive these sim expressions, we start from a complete one-loop EW order calculation, and then take the high energy limit using [9]. As in the analogous cases studied in [10,11], these expressions constitute a very good high energy approximation, to the HC amplitudes, renormalized on shell [16].

Apart from possible additive constants, these sim expressions consist of linear combinations of just four forms [10,11]. For $e^-e^+ \to W^-W^+$, the structure of these forms simplifies as

$$\overline{\ln^2 x_{Vi}} = \ln^2 x_V + 4L_{aVi}, \qquad x_V \equiv \left(\frac{-x - i\epsilon}{m_V^2}\right), \tag{A1}$$

$$\overline{\ln x_{ij}} = \ln x_{ij} + b_0^{ij}(m_a^2) - 2, \quad \ln x_{ij} \equiv \ln \frac{-x - i\epsilon}{m_i m_j}, \tag{A2}$$

$$\overline{\ln^2 r_{xy}} = \ln^2 r_{xy} + \pi^2, \qquad r_{xy} \equiv \frac{-x - i\epsilon}{-y - i\epsilon}, \tag{A3}$$

$$\ln r_{xy}, \tag{A4}$$

where (x, y) denotes any two of the Mandelstam variables (s, t, u).

The indices (i, j, V) in the first two forms, (A1) and (A2), called Sudakov augmented forms [10], denote internally exchanged particles in the various one-loop diagrams, while V always refers to a gauge exchange. The index "a" always refers to a particle such that the tree-level vertices aVi or aij are nonvanishing. This particle a, could either be an external particle (i.e., $e^{\mp}$ or $W^{\mp}$ for the process studied here), or a particle contributing at tree level through an exchange in the s, t, or u channels (i.e., ν_e, or[5] γ, Z in our case). Using these, the energy-independent expressions in (A1) and (A2) may be written as [9–11]

[5]As always, for an internal photon we use a mass m_γ, in order to regularize possible infrared singularities.

$$L_{aVi} = \mathrm{Li}_2\left(\frac{2m_a^2 + i\epsilon}{m_V^2 - m_i^2 + m_a^2 + i\epsilon + \sqrt{\lambda(m_a^2 + i\epsilon, m_V^2, m_i^2)}}\right) + \mathrm{Li}_2\left(\frac{2m_a^2 + i\epsilon}{m_V^2 - m_i^2 + m_a^2 + i\epsilon - \sqrt{\lambda(m_a^2 + i\epsilon, m_V^2, m_i^2)}}\right), \tag{A5}$$

$$b_0^{ij}(m_a^2) \equiv b_0(m_a^2; m_i, m_j) = 2 + \frac{1}{m_a^2}\left[(m_j^2 - m_i^2)\ln\frac{m_i}{m_j} + \sqrt{\lambda(m_a^2 + i\epsilon, m_i^2, m_j^2)}\,\mathrm{ArcCosh}\left(\frac{m_i^2 + m_j^2 - m_a^2 - i\epsilon}{2m_i m_j}\right)\right], \tag{A6}$$

where

$$\lambda(a, b, c) = a^2 + b^2 + c^2 - 2ab - 2ac - 2bc. \tag{A7}$$

The other two forms, (A3) and (A4) are solely induced by box contributions to the asymptotic amplitudes [9]. The forms (A4), in particular, have no dependence on mass scales and never arise from differences of the augmented Sudakov linear-log contributions, of the type (A2).

As already said, apart from possible additive constants, the sim expressions consist of linear combinations of the four forms (A1)–(A4). The coefficients of these forms may involve ratios of Mandelstam variables, as well as constants. Particularly for the Sudakov augmented forms, (A1) and (A2), though, their coefficients should be such that, when differences in the scales of masses and Mandelstam variables are disregarded then, the complete coefficients in the implied, e.g., $\ln s$ and $\ln^2 s$ terms become the constants given by general rules [25–28].

Generally, these supersimple HC helicity amplitudes differ from the on-shell renormalized ones [16] by small additive constant terms in both the MSSM and SM cases. We have checked numerically that for the process studied here, these are indeed negligible.

In the next two subsections we give the supersimple expressions for the $e^-e^+ \to W_T^- W_T^+$ and $e^-e^+ \to W_L^- W_L^+$ HC amplitudes, respectively. In these, we first give the results for the case where infrared singularities are regularized by using $m_\gamma = m_Z$ [10,11] and subsequently quote the corrections for the $m_\gamma \neq m_Z$ case. In each case we give separately the SM and the MSSM predictions.

1. The $e^-e^+ \to W_T^- W_T^+$ HC amplitudes

There are two such HC amplitudes listed in the left part of (7), namely, $F_{-\frac{1}{2}-+}$ and $F_{-\frac{1}{2}+-}$. In the $m_\gamma = m_Z$ case, using the Born results in (13), the asymptotic sim SM expressions are

$$\begin{aligned}
F_{-\frac{1}{2}-+} = {} & F^{\mathrm{Born}}_{-\frac{1}{2}-+}\left(\frac{\alpha}{16\pi s_W^2}\right)\Bigg\{\overline{\ln t_{Ze}}\left(\frac{3 + 2c_W^2}{c_W^2} - \frac{4t}{s} + \frac{4s}{u}\right) + \overline{\ln t_{W\nu}}\left(\frac{-1 + 10c_W^2}{c_W^2} - \frac{8t}{s}\right) + \frac{\overline{\ln t_{Z\nu}}}{c_W^2} + 2\overline{\ln t_{We}} + \overline{\ln u_{Ze}}\left(\frac{4t}{u} - \frac{4t}{s}\right) \\
& + \frac{8t}{s}(\overline{\ln s_{W\nu}} + \overline{\ln s_{Ze}}) - 4\overline{\ln u_{W\nu}} - 3\overline{\ln^2 t_{Ze}} - \overline{\ln^2 t_{ZW}} - 3\overline{\ln^2 t_{W\nu}} - \overline{\ln^2 t_{WZ}} - \frac{1}{c_W^2}(\overline{\ln^2 s_{Ze}} + 4c_W^2\overline{\ln^2 s_{ZW}}) \\
& - 2\overline{\ln^2 s_{WZ}} + 2\overline{\ln^2 u_{Ze}} + 2\overline{\ln^2 u_{ZW}} - \frac{2t}{u}(\overline{\ln^2 s_{W\nu}} + \overline{\ln^2 s_{WZ}} - \overline{\ln^2 t_{W\nu}} - \overline{\ln^2 t_{WZ}}) \\
& + \overline{\ln^2 r_{ts}}\left[\frac{2u^3 + 2t^3 + 6ut^2 + 2tu^2)}{2u^3 c_W^2} + \frac{6u^3 - 6t^3)}{u^3}\right] + \frac{4s}{u}\overline{\ln^2 r_{ut}} + \frac{4(t-u)}{u}\overline{\ln^2 r_{us}} \\
& + \left[\frac{t(2t + 5u)}{u^2 c_W^2} + \frac{t(12t^2 + 6u^2 + 6tu)}{su^2}\right]\ln r_{ts} + \frac{t(16u + 12t)}{su}\ln r_{us} - \left(\frac{8t}{u} + 4\right)\ln r_{tu} + \frac{t(1 - 6c_W^2)}{uc_W^2}\Bigg\},
\end{aligned} \tag{A8}$$

$$\begin{aligned}
F_{-\frac{1}{2}+-} = {} & F^{\mathrm{Born}}_{-\frac{1}{2}+-}\left(\frac{\alpha}{16\pi s_W^2}\right)\Bigg\{\overline{\ln t_{Ze}}\left(\frac{3 + 2c_W^2}{c_W^2} - \frac{4t}{s} + \frac{4s}{u}\right) + \overline{\ln t_{W\nu}}\left(\frac{-1 + 10c_W^2}{c_W^2} - \frac{8t}{s}\right) + \frac{1}{c_W^2}\overline{\ln t_{Z\nu}} + 2\overline{\ln t_{We}} \\
& + \overline{\ln u_{Ze}}\left(\frac{4t}{u} - \frac{4t}{s}\right) + \frac{8t}{s}(\overline{\ln s_{W\nu}} + \overline{\ln s_{Ze}}) - 4\overline{\ln u_{W\nu}} - 3\overline{\ln^2 t_{Ze}} - \overline{\ln^2 t_{ZW}} - 3\overline{\ln^2 t_{W\nu}} - \overline{\ln^2 t_{WZ}} \\
& - \frac{1}{c_W^2}(\overline{\ln^2 s_{Ze}} + 4c_W^2\overline{\ln^2 s_{ZW}}) - 2\overline{\ln^2 s_{WZ}} + 2\overline{\ln^2 u_{Ze}} + 2\overline{\ln^2 u_{ZW}} - \frac{2t}{u}(\overline{\ln^2 s_{W\nu}} + \overline{\ln^2 s_{WZ}} - \overline{\ln^2 t_{W\nu}} - \overline{\ln^2 t_{WZ}}) \\
& + \overline{\ln^2 r_{ts}}\left[\frac{u - t}{uc_W^2} + \frac{6(u - t)}{u}\right] + \frac{4s}{u}\overline{\ln^2 r_{ut}} + \left(\frac{4t^2 + 2ut + 6u^2}{ut}\right)\overline{\ln^2 r_{us}} + \left[\frac{-3}{c_W^2} + \frac{18u^2 + 30ut}{su}\right]\ln r_{ts} \\
& + \left(\frac{4t}{u} + 8\right)\ln r_{tu} + \left(\frac{4t}{s} + 12\right)\ln r_{us} - \frac{1 - 6c_W^2}{c_W^2}\Bigg\},
\end{aligned} \tag{A9}$$

while the sim MSSM results, always assuming CP conservation, are

$$F_{-\frac{1}{2}-+} = F^{\text{Born}}_{-\frac{1}{2}-+}\left(\frac{\alpha}{16\pi s_W^2}\right)\Big\{\frac{1}{c_W^2}(3\overline{\ln t_{Ze}} - \overline{\ln t_{W\nu}} + \overline{\ln t_{Z\nu}}) - 2\overline{\ln t_{Ze}} + 6\overline{\ln t_{W\nu}} + 2\overline{\ln t_{We}} - 3\overline{\ln^2 t_{Ze}} - \overline{\ln^2 t_{ZW}} - 3\overline{\ln^2 t_{W\nu}}$$
$$- \overline{\ln^2 t_{WZ}} - \frac{1}{c_W^2}(\overline{\ln^2 s_{Ze}} + 4c_W^2\overline{\ln^2 s_{ZW}}) - 2\overline{\ln^2 s_{WZ}} + 2\overline{\ln^2 u_{Ze}} + 2\overline{\ln^2 u_{ZW}} - \frac{2t}{u}(\overline{\ln^2 s_{W\nu}} + \overline{\ln^2 s_{WZ}} - \overline{\ln^2 t_{W\nu}} - \overline{\ln^2 t_{WZ}})$$
$$+ \frac{4s}{u}\ln r_{tu} - \frac{12t^2}{su}\ln r_{ts} + \left(\frac{4t}{s} - \frac{8t}{u}\right)\ln r_{us} + \frac{2t}{uc_W^2}\ln r_{ts} - \frac{1}{c_W^2}\Big\{\sum_j |Z^N_{1j}s_W + Z^N_{2j}c_W|^2\overline{\ln t_{\chi^0_j\tilde{e}_L}} + 2c_W^2\sum_j |Z^+_{1j}|^2\overline{\ln t_{\chi^+_j\tilde{\nu}}}\Big\}$$
$$+ \overline{\ln^2 r_{ts}}\left[\frac{t^2+u^2}{u^2c_W^2} + \frac{6t^2+6u^2)}{u^2}\right] + \frac{4s}{u}\overline{\ln^2 r_{ut}} + \frac{4(t-u)}{u}\overline{\ln^2 r_{us}}\Big\}, \tag{A10}$$

$$F_{-\frac{1}{2}+-} = F^{\text{Born}}_{-\frac{1}{2}+-}\left(\frac{\alpha}{16\pi s_W^2}\right)\Big\{\frac{1}{c_W^2}[3\overline{\ln t_{Ze}} - \overline{\ln t_{W\nu}} + \overline{\ln t_{Z\nu}}] - 2\overline{\ln t_{Ze}} + 6\overline{\ln t_{W\nu}} + 2\overline{\ln t_{We}} - 3\overline{\ln^2 t_{Ze}} - \overline{\ln^2 t_{ZW}} - 3\overline{\ln^2 t_{W\nu}}$$
$$- \overline{\ln^2 t_{WZ}} - \frac{1}{c_W^2}(\overline{\ln^2 s_{Ze}} + 4c_W^2\overline{\ln^2 s_{ZW}}) - 2\overline{\ln^2 s_{WZ}} + 2\overline{\ln^2 u_{Ze}} + 2\overline{\ln^2 u_{ZW}} - \frac{2t}{u}(\overline{\ln^2 s_{W\nu}} + \overline{\ln^2 s_{WZ}} - \overline{\ln^2 t_{W\nu}} - \overline{\ln^2 t_{WZ}})$$
$$+ \frac{12(t-s)}{s}\ln r_{ts} + \left(\frac{4t}{s} + 8\right)\ln r_{us} - \left(\frac{2}{c_W^2}\right)\ln r_{ts} - \frac{4s}{u}\ln r_{tu} - \frac{1}{c_W^2}\Big\{\sum_j |Z^N_{1j}s_W + Z^N_{2j}c_W|^2\overline{\ln t_{\chi^0_j\tilde{e}_L}}$$
$$+ 2c_W^2\sum_j |Z^+_{1j}|^2\overline{\ln t_{\chi^+_j\tilde{\nu}}}\Big\} + \overline{\ln^2 r_{ts}}\left[\frac{u-t}{uc_W^2} + \frac{6(u-t)}{u}\right] + \frac{4s}{u}\overline{\ln^2 r_{ut}} + \frac{4(t^2+u^2)}{ut}\overline{\ln^2 r_{us}}\Big\}, \tag{A11}$$

where the indices (i, j) in, (A10), (A11), (A15), and (A16) below, refer to chargino and neutralino contributions, defined as in [29].

Note the constant terms at the end of the rhs of the SM results, (A8) and (A9). No such constants appear in the corresponding MSSM amplitudes, (A10) and (A11).

In the $m_\gamma \neq m_Z$ case, the correction to be added to (A8)–(A11), is given by

$$\delta F_{-\frac{1}{2}\mp\pm} = F^{\text{Born}}_{-\frac{1}{2}\mp\pm}\left(\frac{\alpha}{16\pi s_W^2}\right)\Big[\Big\{-2s_W^2(\overline{\ln^2 t_{\gamma e}} + \overline{\ln^2 t_{\gamma W}}) + 16s_W^2\frac{t}{s}\overline{\ln s_{\gamma e}} + 2s_W^2[-2\overline{\ln^2 s_{\gamma e}} + 8\overline{\ln t_{\gamma e}}]$$
$$- 2s_W^2[2\overline{\ln^2 s_{\gamma W}} + \overline{\ln^2 t_{W\gamma}}] + 2s_W^2[-2\overline{\ln^2 s_{W\gamma}} - \overline{\ln^2 t_{\gamma e}} - \overline{\ln^2 t_{\gamma W}} + 4\left(1 - \frac{t}{s}\right)\overline{\ln t_{\gamma e}}\Big]$$
$$+ 2s_W^2\Big[-2\frac{t}{u}\overline{\ln^2 s_{W\gamma}} - \frac{t}{u}(\overline{\ln^2 u_{\gamma e}} + \overline{\ln^2 u_{\gamma W}}) + 4\left(\frac{t}{u} - \frac{t}{s}\right)\overline{\ln u_{\gamma e}}\Big] - 2s_W^2\Big[\frac{s-u}{u}\left(\overline{\ln^2 u_{\gamma e}} + \overline{\ln^2 u_{\gamma W}}\right)$$
$$+ \frac{s-t}{u}\overline{\ln^2 t_{W\gamma}} + 4\left(2 + \frac{t}{u}\right)\overline{\ln t_{\gamma e}}\Big]\Big\} - \{m_\gamma \to m_Z\}\Big], \tag{A12}$$

where (13) is again used.

2. The $e^-e^+ \to W_L^-W_L^+$ HC amplitudes

In the $m_\gamma = m_Z$ case, using the asymptotic Born LL amplitudes (17), the high energy sim SM results are written as

$$F_{+\frac{1}{2}00} = F^{\text{Born}}_{+\frac{1}{2}00}\Big\{\left(\frac{\alpha}{4\pi}\right)\Big\{\frac{1}{c_W^2}[-\overline{\ln^2 s_{Ze}} + 3\overline{\ln s_{Ze}} - 1] + \frac{1}{4s_W^2c_W^2}[-\overline{\ln^2 s_{ZW}} + 4\overline{\ln s_{ZW}}]$$
$$+ \frac{1}{2s_W^2}\Big[-\frac{1}{2}(\overline{\ln^2 s_{WZ}} + \overline{\ln^2 s_{WH_{\text{SM}}}}) + 2\overline{\ln s_{WZ}} + 2\overline{\ln s_{WH_{\text{SM}}}}\Big] - \frac{3(m_t^2+m_b^2)}{2s_W^2m_W^2}\overline{\ln s_{tb}}$$
$$- \frac{1}{4c_W^2}\Big[4(\overline{\ln^2 t_{ZW}} - \overline{\ln^2 u_{ZW}}) + \frac{2(u-t)}{u}\overline{\ln^2 r_{ts}} - \frac{2(t-u)}{t}\overline{\ln^2 r_{us}}\Big]\Big\} + \Sigma^{\text{seSM}}\left(+\frac{1}{2}, 0, 0\right)\Big\}, \tag{A13}$$

$$F_{-\frac{1}{2}00} = F^{\rm Born}_{-\frac{1}{2}00}\Bigg\{\left(\frac{\alpha}{4\pi}\right)\Bigg\{\frac{1}{4s_W^2c_W^2}[-\overline{\ln^2 s_{Ze}} + 3\overline{\ln s_{Ze}} - 1] - \frac{(1-2s_W^2)}{2s_W^2}[-\overline{\ln^2 s_{W\nu}} + 3\overline{\ln s_{W\nu}} - 1] + \frac{2c_W^2}{s_W^2}\Bigg[\frac{1}{2}\overline{\ln s_{W\nu}}$$
$$+ \frac{1}{2} + 2\overline{\ln s_{WW}}\Bigg] + \frac{1}{4s_W^2c_W^2}[-\overline{\ln^2 s_{ZW}} + 4\overline{\ln s_{ZW}}] + \frac{(1-2c_W^2)}{2s_W^2}\Bigg[-\frac{1}{2}(\overline{\ln^2 s_{WZ}} + \overline{\ln^2 s_{WH_{\rm SM}}}) + 2\overline{\ln s_{WZ}} + 2\overline{\ln s_{WH_{\rm SM}}}\Bigg]$$
$$+ \frac{c_W^2}{s_W^2}[\overline{\ln s_{WZ}} + \overline{\ln s_{WH_{SM}}}] - \frac{3(m_t^2+m_b^2)}{2s_W^2m_W^2}\overline{\ln s_{tb}} - \frac{c_W^2}{4s_W^2}\Bigg[4\overline{\ln^2 t_{W\nu}} + 2\overline{\ln^2 t_{WZ}} + 2\overline{\ln^2 t_{WH_{\rm SM}}} - 4\left(1-\frac{t}{u}\right)\overline{\ln^2 r_{ts}}\Bigg]$$
$$- \frac{1}{8c_W^2s_W^2}\Bigg[4(\overline{\ln^2 t_{ZW}} - \overline{\ln^2 u_{ZW}}) + \frac{2(u-t)}{u}\overline{\ln^2 r_{ts}} - \frac{2(t-u)}{t}\overline{\ln^2 r_{us}}\Bigg]\Bigg\} + \Sigma^{\rm seSM}\left(-\frac{1}{2},0,0\right)\Bigg\}, \tag{A14}$$

while the sim MSSM results are

$$F_{+\frac{1}{2}00} = F^{\rm Born}_{+\frac{1}{2}00}\Bigg\{\left(\frac{\alpha}{4\pi}\right)\Bigg\{\frac{1}{c_W^2}[-\overline{\ln^2 s_{Ze}} + 3\overline{\ln s_{Ze}} - \Sigma_i|Z^N_{1i}|^2\overline{\ln s_{\chi_i^0\tilde{e}_R}}] + \frac{1}{4s_W^2c_W^2}[-\overline{\ln^2 s_{ZW}} + 4\overline{\ln s_{ZW}}]$$
$$+ \frac{1}{2s_W^2}\Bigg[-\frac{1}{2}\overline{\ln^2 s_{WZ}} + 2\overline{\ln s_{WZ}}\Bigg] - \frac{1}{4s_W^2}[\cos^2(\beta-\alpha)\overline{\ln^2 s_{WH^0}} + \sin^2(\beta-\alpha)\overline{\ln^2 s_{Wh^0}}]$$
$$+ \frac{1}{2s_W^2}[2\cos^2(\beta-\alpha)\overline{\ln s_{WH^0}} + 2\sin^2(\beta-\alpha)\overline{\ln s_{Wh^0}}] - \frac{1}{2s_W^2c_W^2}\Sigma_{ij}\Bigg[\left|\frac{1}{\sqrt{2}}Z^-_{2i}(Z^N_{1j}s_W + Z^N_{2j}c_W) - Z^-_{1i}Z^N_{3j}c_W\right|^2$$
$$+ \left|\frac{1}{\sqrt{2}}Z^+_{2i}(Z^N_{1j}s_W + Z^N_{2j}c_W) + Z^+_{1i}Z^N_{4j}c_W\right|^2\Bigg]\overline{\ln s_{\chi_i^+\chi_j^0}} - \frac{3(m_t^2+m_b^2)}{2s_W^2m_W^2}\overline{\ln s_{tb}} - \frac{\cos^2\beta}{2c_W^2}\Bigg[\frac{s}{u}\overline{\ln^2 r_{ts}} - \frac{s}{t}\overline{\ln^2 r_{us}}\Bigg]$$
$$- \frac{1}{4c_W^2}\Bigg[4(\overline{\ln^2 t_{ZW}} - \overline{\ln^2 u_{ZW}}) + \frac{2(u-t)}{u}\overline{\ln^2 r_{ts}} - \frac{2(t-u)}{t}\overline{\ln^2 r_{us}}\Bigg]\Bigg\} + \Sigma^{\rm seMSSM}\left(+\frac{1}{2},0,0\right)\Bigg\}, \tag{A15}$$

$$F_{-\frac{1}{2}00} = F^{\rm Born}_{-\frac{1}{2}00}\Bigg\{\left(\frac{\alpha}{4\pi}\right)\Bigg\{\frac{1}{4s_W^2c_W^2}[-\overline{\ln^2 s_{Ze}} + 3\overline{\ln s_{Ze}} - \overline{\ln^2 s_{ZW}} + 4\overline{\ln s_{ZW}} - \Sigma_i|Z^N_{1i}s_W + Z^N_{2i}c_W|^2\overline{\ln s_{\chi_i^0\tilde{e}_L}}]$$
$$- \frac{(1-2s_W^2)}{2s_W^2}\Bigg[-\overline{\ln^2 s_{W\nu}} + 3\overline{\ln s_{W\nu}} - \frac{1}{2}\overline{\ln^2 s_{WZ}} + 2\overline{\ln s_{WZ}} - \Sigma_i|Z^+_{1i}|^2\overline{\ln s_{\chi_i^+\tilde{\nu}_L}}\Bigg] + \frac{c_W^2}{s_W^2}[\overline{\ln s_{W\nu}} + 4\overline{\ln s_{WW}}$$
$$- \Sigma_i|Z^+_{1i}|^2\overline{\ln s_{\chi_i^+\tilde{\nu}_L}}] - \frac{(1-2c_W^2)}{4s_W^2}[\cos^2(\beta-\alpha)\overline{\ln^2 s_{WH^0}} + \sin^2(\beta-\alpha)\overline{\ln^2 s_{Wh^0}}] + \frac{(1-2c_W^2)}{s_W^2}[\cos^2(\beta-\alpha)\overline{\ln s_{WH^0}}$$
$$+ \sin^2(\beta-\alpha)\overline{\ln s_{Wh^0}}] + \frac{c_W^2}{s_W^2}[\overline{\ln s_{WZ}} + \cos^2(\beta-\alpha)\overline{\ln s_{WH^0}} + \sin^2(\beta-\alpha)\overline{\ln s_{Wh^0}}] - \frac{3(m_t^2+m_b^2)}{2s_W^2m_W^2}\overline{\ln s_{tb}}$$
$$- \frac{1}{2s_W^2c_W^2}\Sigma_{ij}\Bigg[\left|\frac{1}{\sqrt{2}}Z^-_{2i}(Z^N_{1j}s_W + Z^N_{2j}c_W) - Z^-_{1i}Z^N_{3j}c_W\right|^2 + \left|\frac{1}{\sqrt{2}}Z^+_{2i}(Z^N_{1j}s_W + Z^N_{2j}c_W) + Z^+_{1i}Z^N_{4j}c_W\right|^2\Bigg]\overline{\ln s_{\chi_i^+\chi_j^0}}$$
$$- \frac{c_W^2}{4s_W^2}\Bigg[4\overline{\ln^2 t_{W\nu}} + 2\overline{\ln^2 t_{WZ}} - 4\left(1-\frac{t}{u}\right)\overline{\ln^2 r_{ts}}\Bigg] - \frac{c_W^2}{2s_W^2}[\cos^2(\beta-\alpha)\overline{\ln^2 t_{WH^0}} + \sin^2(\beta-\alpha)\overline{\ln^2 t_{Wh^0}}]$$
$$- \frac{1}{8c_W^2s_W^2}\Bigg[4(\overline{\ln^2 t_{ZW}} - \overline{\ln^2 u_{ZW}}) + \frac{2(u-t)}{u}\overline{\ln^2 r_{ts}} - \frac{2(t-u)}{t}\overline{ln^2 r_{us}}\Bigg] - \frac{\sin^2\beta}{2c_W^2s_W^2}\Bigg[\frac{s}{u}\overline{\ln^2 r_{ts}} - \frac{s}{t}\overline{\ln^2 r_{us}}\Bigg]$$
$$- \frac{c_W^2\sin^2\beta}{s_W^2}\frac{s}{u}\overline{\ln^2 r_{ts}}\Bigg\} + \Sigma^{\rm seMSSM}\left(-\frac{1}{2},0,0\right)\Bigg\}. \tag{A16}$$

In the $m_\gamma \neq m_Z$ case, the correction to be added to (A13)–(A16) is given by

$$\delta F_{\pm\frac{1}{2}00} = F^{\rm Born}_{\pm\frac{1}{2}00}\left(\frac{\alpha}{4\pi}\right)[\{-\overline{\ln^2 s_{\gamma e}} + 3\overline{\ln s_{\gamma e}} - \overline{\ln^2 s_{\gamma W}} + 4\overline{\ln s_{\gamma W}} - 2\overline{\ln^2 t_{\gamma W}} + 2\overline{\ln^2 u_{\gamma W}}\} - \{m_\gamma \to m_Z\}], \tag{A17}$$

where (17) is again used.

The Σ^{se} contributions in either (A13) and (A14) or (A15) and (A16), respectively, appearing in SM and MSSM, come from the photon and Z self-energy contributions together with their renormalization counterterms. Their explicit expressions are

$$\Sigma^{se}\left(-\frac{1}{2},0,0\right)=\frac{-4s_W^2c_W^2}{s}\left\{\hat{\Sigma}_{\gamma\gamma}(s)+\frac{1-2s_W^2}{s_Wc_W}\hat{\Sigma}_{Z\gamma}(s)+\frac{(1-2s_W^2)^2}{4s_W^2c_W^2}\hat{\Sigma}_{ZZ}(s)\right\}+C_P, \tag{A18}$$

$$\Sigma^{se}\left(+\frac{1}{2},0,0\right)=\frac{-2c_W^2}{s}\left\{\hat{\Sigma}_{\gamma\gamma}(s)+\frac{1-4s_W^2}{2s_Wc_W}\hat{\Sigma}_{Z\gamma}(s)-\frac{(1-2s_W^2)}{2c_W^2}\hat{\Sigma}_{ZZ}(s)\right\}, \tag{A19}$$

where the renormalized gauge self-energies $\hat{\Sigma}$ can be found in [11], together with their supersimple approximations. The last term in (A18), given by

$$C_P=-\frac{\alpha c_W^2}{\pi s_W^2}\overline{\ln s_{WW}}, \tag{A20}$$

comes from the pinch part that had been previously removed from the left and right triangular contributions, and is here restored [30,31].

Note that no such Σ^{se} contributions exist for the transverse amplitudes in (A8)–(A11).

As it should, the high energy ln and ln-squared parts of all expressions (A8)–(A11), agree with the usual Sudakov rules and the renormalization group results

$$A^{RG}=-\frac{ln}{4\pi^2}\left(g^4\beta\frac{dA^{\rm Born}}{dg^2}+g^{-4}\beta'\frac{dA^{\rm Born}}{dg'^2}\right),\qquad \beta^{\rm SM}=\frac{43}{24}-\frac{N_f}{3},\qquad \beta^{\rm SUSY}=-\frac{13}{24}-\frac{N_f}{6},$$
$$N_f=3,\qquad \beta'^{\rm SM}=-\frac{1}{24}-\frac{5N_f}{9},\qquad \beta'^{\rm SUSY}=-\frac{5}{24}-\frac{5N_f}{18}, \tag{A21}$$

discussed in [25–28].

APPENDIX B: AGC AND Z' AMPLITUDES

1. The AGC amplitudes

As an AGC model induced by the s-channel γ and Z exchanges with five anomalous couplings δ_Z, $x_{\gamma,Z}$, $y_{\gamma,Z}$, we consider the one presented in [32] and Table V of [12]. In terms of these couplings and the SM ones in (10), the induced AGC contributions to the TT, TL, LT, and LL amplitudes, to lowest order, are[6]

$$F^{\rm AGC}_{\lambda\mu\mu}(\theta)=\frac{(2\lambda)se^2}{8}(1+\mu\mu')\beta_W\sin\theta\left\{\frac{\delta_Z(a_{eL}\delta_{\lambda,-}+a_{eR}\delta_{\lambda,+})}{s_W^2(s-m_Z^2)}-\left[\frac{y_\gamma}{s}-\frac{y_Z(a_{eL}\delta_{\lambda,-}+a_{eR}\delta_{\lambda,+})}{2s_W^2(s-m_Z^2)}\right]\frac{s}{m_W^2}\right\}, \tag{B1}$$

$$F^{\rm AGC}_{\lambda\mu0}(\theta)=-\frac{(2\lambda)s\beta_W\sqrt{s}e^2}{4\sqrt{2}m_W}(2\lambda+\mu\cos\theta)\left\{\frac{\delta_Z(a_{eL}\delta_{\lambda,-}+a_{eR}\delta_{\lambda,+})}{s_W^2(s-m_Z^2)}-\left[\frac{(x_\gamma+y_\gamma)}{s}-\frac{(x_Z+y_Z)(a_{eL}\delta_{\lambda,-}+a_{eR}\delta_{\lambda,+})}{2s_W^2(s-m_Z^2)}\right]\right\}, \tag{B2}$$

$$F^{\rm AGC}_{\lambda0\mu'}(\theta)=-\frac{(2\lambda)s\beta_W\sqrt{s}e^2}{4\sqrt{2}m_W}(2\lambda-\mu'\cos\theta)\left\{\frac{\delta_Z(a_{eL}\delta_{\lambda,-}+a_{eR}\delta_{\lambda,+})}{s_W^2(s-m_Z^2)}-\left[\frac{(x_\gamma+y_\gamma)}{s}-\frac{(x_Z+y_Z)(a_{eL}\delta_{\lambda,-}+a_{eR}\delta_{\lambda,+})}{2s_W^2(s-m_Z^2)}\right]\right\}, \tag{B3}$$

$$F^{\rm AHC}_{\lambda00}(\theta)=\frac{(2\lambda)s^2e^2}{4m_W^2}\beta_W\sin\theta\left\{\frac{\delta_Z(a_{eL}\delta_{\lambda,-}+a_{eR}\delta_{\lambda,+})}{s_W^2(s-m_Z^2)}\left(1+\frac{s}{2m_W^2}\right)-\left[\frac{x_\gamma}{s}-x_Z\frac{a_{eL}\delta_{\lambda,-}+a_{eR}\delta_{\lambda,+}}{2s_W^2(s-m_Z^2)}\right]\frac{s}{m_W^2}\right\}. \tag{B4}$$

[6]Compare with (9) and (14)–(16).

Note that δ_Z contributes to all amplitudes, except the two TT HC ones [because of the vanishing of the overall coefficient $(1 + \mu\mu')$ in (B1) in such a case]; $x_{\gamma,Z}$ contribute to all TL, LT, and LL amplitudes, while $y_{\gamma,Z}$ contribute only to the HV TT, TL, and LT amplitudes.

In the figures, and under the name AGC1, we present illustrations for the purely arbitrary choice

$$\text{AGC1} \Rightarrow \delta_Z = x_\gamma = x_Z = 0.003, \qquad y_\gamma = y_Z = 0. \tag{B5}$$

For AGC1, the HV TT anomalous amplitudes behave like constants at high energy; the HC LL ones explode like s/m_W^2, while the LT ones increase like $\sqrt{s}/m_W^2$.

In the figures we also present results for an alternative AGC2 model in which the s/m_W^2 behavior of the HC LL anomalous amplitudes is canceled by a t-channel contribution, much like it is done in the Born SM case. So we construct an *ad hoc* model with an anomalous contribution in the t channel which would lead to a similar cancellation. A simple phenomenological solution is obtained by keeping only x_γ and x_Z (called now x'_γ and x'_Z) in (B1)–(B4), and adding t-channel contributions induced by left- and right-handed $We\nu$ couplings obtained from the initial SM one $g_L = e/(\sqrt{2}s_W)$, through

$$\begin{aligned} g_L^2 &\Rightarrow g_L^2\left(1 + 2s_W^2\left[x'_\gamma - \frac{2s_W^2 - 1}{2s_W c_W}x'_Z\right]\right), \\ g_R^2 &\Rightarrow g_L^2(2s_W^2)\left[x'_\gamma - \frac{s_W}{c_W}x'_Z\right]. \end{aligned} \tag{B6}$$

This does not necessarily represent true anomalous $We\nu$ couplings; it just represents the new contribution necessary at high energy. For example, it may come from additional neutral fermion exchanges or from any sort of effective interaction. In the illustrations under the AGC2 name, we use

$$\text{AGC2} \Rightarrow x'_\gamma = x'_Z = 0.03; \tag{B7}$$

these values are larger than those in (B5) because of the global suppression effect following from the high energy cancellation between t- and s-channel terms.

If one does not want to introduce an anomalous right-handed contribution one can just keep a nonvanishing x'_γ only and add the anomalous left-handed term

$$g_L^2 \Rightarrow g_L^2(1 + 2s_W^2 x'_\gamma). \tag{B8}$$

In any case, investigating the origin of such anomalous terms is beyond the scope of the present work.

2. The Z' new physics model

The general form of helicity amplitudes with a Z' is written in Table VI of [12]. The Z' contributions are very similar to the SM Z ones, with specific Z' mass, width, and couplings.

In general, with arbitrary Z' couplings, there is an explosion of the LL, LT, and TL amplitudes at high energies. But, it is again easy to get high energy cancellation in an *ad hoc* manner by just replacing the usual Z contribution involving products of couplings like $g_{Zee}g_{ZWW}$, by $Z + Z'$ exchanges using, respectively, $g_{Zee}g_{ZWW}\cos^2\Phi$ for Z and $g_{Zee}g_{ZWW}\sin^2\Phi$ for Z' (with a small value of Φ). This way, the s-channel high energy contribution will be similar to the SM Z one, and will cancel with the SM t-channel contribution. Only around the Z' peak will the Z' contribution be observable.

For the illustrations presented in the figures under the name Z', we use $\sin\Phi = 0.05$ and $m_{Z'} = 3$ TeV.

[1] M. Böhm, A. Denner, T. Sack, W. Beenakker, F. Berends, and H. Kuijf, Nucl. Phys. **B304**, 463 (1988).
[2] W. Beenakker and A. Denner, Int. J. Mod. Phys. A **09**, 4837 (1994).
[3] T. Hahn, Nucl. Phys. **B609**, 344 (2001).
[4] A. Denner, S. Dittmaier, M. Roth, and L. H. Wieders, Nucl. Phys. **B724**, 247 (2005).
[5] ALEPH, DELPHI, L3, OPAL Collaborations, and LEP Working Group, Phys. Rep. **532**, 119 (2013).
[6] ATLAS Collaboration, Phys. Rev. D **87**, 112001 (2013); CMS Collaboration, Eur. Phys. J. C **73**, 2610 (2013).
[7] Ties Behnke *et al.*, arXiv:1306.6327; C. Adolphsen *et al.*, arXiv:1306.6352; arXiv:1306.6353; arXiv:1306.6328; T. Behnke *et al.*, arXiv:1306.6329.
[8] P. Lebrun *et al.*, Report No. CERN-2012-005; H. Abramowicz *et al.*, arXiv:1307.5288.
[9] M. Beccaria, G. J. Gounaris, J. Layssac, and F. M. Renard, Int. J. Mod. Phys. A **23**, 1839 (2008).
[10] G. J. Gounaris and F. M. Renard, Acta Phys. Pol. B **42**, 2107 (2011).
[11] G. J. Gounaris and F. M. Renard, Phys. Rev. D **86**, 013003 (2012).
[12] V. V. Andreev, G. Moorgat-Pick, P. Osland, A. A. Pankov, and N. Paver, Eur. Phys. J. C **72**, 2147 (2012).
[13] G. J. Gounaris and F. M. Renard, Phys. Rev. Lett. **94**, 131601 (2005).
[14] G. J. Gounaris and F. M. Renard, Phys. Rev. D **73**, 097301 (2006).
[15] M. Jacob and G. C. Wick, Ann. Phys. (N.Y.) **7**, 404 (1959); **281**, 774 (2000).
[16] W. Hollik, Fortschr. Phys. **38**, 165 (1990).
[17] G. Passarino and M. Veltman, Nucl. Phys. **B160**, 151 (1979).

[18] G. J. Gounaris, C. Le Mouel, and P. I. Porfyriadis, Phys. Rev. D **65**, 035002 (2002).
[19] J. M. Cornwall, D. N. Levin, and G. Tiktopoulos, Phys. Rev. D **10**, 1145 (1974); C. E. Vayonakis, Lett. Nuovo Cimento **17**, 383 (1976); M. S. Chanowitz and M. K. Gaillard, Nucl. Phys. **B261**, 379 (1985); G. J. Gounaris, R. Kögerler, and H. Neufeld, Phys. Rev. D **34**, 3257 (1986).
[20] M. Arana-Catania, S. Heinemeyer, and M. J. Herrero, Phys. Rev. D **88**, 015026 (2013).
[21] M. W. Cahill-Rowley, J. L. Hewett, A. Ismail, M. E. Peskin, and T. G. Rizzo, arXiv:1305.2419.
[22] Y. Konishi, S. Ohta, J. Sato, T. Shimomura, K. Sugal, and M. Yamanaka, arXiv:1309.2067.
[23] G. J. Gounaris and F. M. Renard, Z. Phys. C **59**, 133 (1993).
[24] G. Altarelli, arXiv:1308.0545.
[25] M. Beccaria, F. M. Renard, and C. Verzegnassi, Linear Collider Note No. LC-TH-2002-005; GDR Supersymmetrie Note No. GDR-S-081.
[26] M. Beccaria, M. Melles, F. M. Renard, S. Trimarchi, and C. Verzegnassi, Int. J. Mod. Phys. A **18**, 5069 (2003).
[27] M. Beccaria, F. M. Renard, and C. Verzegnassi, Nucl. Phys. **B663**, 394 (2003).
[28] M. Beccaria and E. Mirabella, Phys. Rev. D **71**, 115016 (2005).
[29] J. Rosiek, Phys. Rev. D **41**, 3464 (1990); corrected by an erratum; the results are given in arXiv:hep-ph/9511250.
[30] G. Degrassi and A. Sirlin, Nucl. Phys. **B383**, 73 (1992); Phys. Rev. D **46**, 3104 (1992).
[31] D. Binosi and J. Papavassiliou, Phys. Rep. **479**, 1 (2009).
[32] G. Gounaris *et al.*, Report No. DESY 92-123B, p. 735; G. Gounaris, J. Layssac, G. Moultaka, and F. M. Renard, Int. J. Mod. Phys. A **08**, 3285 (1993).